9-6-2012

# Oncostatin M Promotes Mammary Tumor Metastasis to Bone and Osteolytic Bone Degradation

Celeste Bolin
*Boise State University*

Ken Tawara
*Boise State University*

Caleb Sutherland
*Boise State University*

Jeff Redshaw
*Boise State University*

Patrick S. Aranda
*Boise State University*

***See next page for additional authors***

**Authors**
Celeste Bolin, Ken Tawara, Caleb Sutherland, Jeff Redshaw, Patrick S. Aranda, Jim Moselhy, Robin Anderson, and Cheryl Jorcyk

DOI: 10.1177/1947601912458284

# Oncostatin M Promotes Mammary Tumor Metastasis to Bone and Osteolytic Bone Degradation

**Celeste Bolin, Ken Tawara, Caleb Sutherland, Jeff Redshaw, Patrick Aranda, and Jim Moselhy**
Boise State University

**Robin Anderson**
The University of Melbourne

**Cheryl L. Jorcyk**
Boise State University

**Abstract**

Oncostatin M (OSM) is an interleukin-6 (IL-6)-family cytokine that has been implicated in a number of biological processes including inflammation, hematopoiesis, immune responses, development, and bone homeostasis. Recent evidence suggests that OSM may promote breast tumor invasion and metastasis. We investigated the role of OSM in the formation of bone metastases *in vivo* using the 4T1.2 mouse mammary tumor model, in which OSM expression was knocked down using shRNA (4T1.2-OSM). 4T1.2-OSM cells were injected orthotopically into Balb/c mice resulting in a greater than 97% decrease in spontaneous metastasis to bone compared to control cells. Intratibial injection of these same 4T1.2-OSM cells also dramatically reduced the osteolytic destruction of trabecular bone volume compared to control cells. Furthermore, in a tumor resection model, mice bearing 4T1.2-OSM tumors showed an increase in survival by a median of 10 days. To investigate the specific cellular mechanisms important for OSM-induced osteolytic metastasis to bone, an *in vitro* model was developed using the RAW 264.7 pre-osteoclast cell line co-cultured with 4T1.2 mouse mammary tumor cells. Treatment of co-cultures with OSM resulted in a 3-fold induction of osteoclastogenesis using the TRAP assay. We identified several tumor cell-induced factors including vascular endothelial growth factor (VEGF), IL-6, and a previously uncharacterized OSM-regulated bone metastasis factor, amphiregulin (AREG), which increased osteoclast differentiation by 4.5-fold. In addition, pre-treatment of co-cultures with an anti-AREG neutralizing antibody completely reversed OSM-induced osteoclastogenesis. Our results suggest that one mechanism for OSM-induced osteoclast differentiation is via an AREG autocrine loop resulting in decreased osteoprotegrin (OPG) secretion by the 4T1.2 cells. These data provide evidence that OSM might be an important therapeutic target for the prevention of breast cancer metastasis to bone.

**Keywords:** oncostatin M, OSM, bone metastasis, breast cancer, osteolysis, osteoclastogenesis

## Introduction

Breast cancer is the most commonly diagnosed cancer in women worldwide, with approximately 200,000 new cases being reported each year in the United States alone (1). Seventy percent of breast cancer patients with advanced disease have bone metastasis. Though not a direct cause of death, these metastases often lead to weakening of weight-bearing bones due to osteolytic lesions, resulting in severe pain, pathologic fractures, and hypercalcemia (2). While mechanisms of breast cancer progression have been researched extensively, metastasis specifically to osseous tissue is understudied, and therefore, the role of inflammatory factors in this process is not well understood. Recent data from human serum samples indicate that the promotion of metastasis to bone may be caused by inflammatory cytokines in the interleukin-6 (IL-6) family (3).

Oncostatin M (OSM) is a pleiotropic IL-6 family cytokine important in inflammation and other cellular processes such as development, hematopoiesis, liver function, neurogenesis, and bone homeostasis (4). OSM activates the JAK/STAT, MAPK, and PI3K/AKT pathways via binding its receptors, OSM receptor beta (OSMRβ) or leukemia inhibitory factor receptor beta (LIFRβ) dimerized with a common gp130 subunit (5-8). During oncogenesis, OSM often acts as an anti-proliferative factor for multiple types of cancers including multiple myeloma, lung cancer, and breast cancer (9, 10). Paradoxically, OSM has also been shown to increase the proliferation of prostate and ovarian cancer cells, although this discrepancy is not well defined (11, 12). Though OSM may promote or inhibit tumor cell proliferation, recent research suggests a contributing role for this cytokine in metastasis (13-16).

In breast cancer, OSM has been shown by our group and others to i) increase the transition of various cancer cell types from an epithelial to a mesenchymal phenotype (EMT) (15), ii) promote breast tumor cell-substrate detachment and invasion *in vitro* (13, 14), iii) upregulate proteases such as matrix metalloproteinases (MMPs) and cathepsins that degrade the local extracellular matrix (unpublished results; (14, 16)), and iv) induce proangiogenic factors such as vascular endothelial growth factor (VEGF) (17, 18). In human tissue, OSM is expressed at low levels in normal mammary epithelial cells and at higher levels in ductal carcinoma *in situ* and invasive breast carcinoma (unpublished results; (19)). High levels of OSM are also found in the breast tumor microenvironment in both tumor-associated macrophages and neutrophils that express and release OSM in response to breast carcinoma cells *in vitro* (20-22). These studies suggest a role for both autocrine and paracrine signaling by OSM in tumor cell detachment and invasion during early stages of the metastatic cascade. The role of OSM in bone colonization and osteolysis has not been addressed previously, but OSM, IL-6, and other gp130-related factors have been shown to regulate normal bone homoeostasis (23-26).

Bone homeostasis is maintained via a constant balance between mineralized bone formation and bone resorption. These processes are mediated primarily by the osteoblasts that synthesize mineralized bone and the osteoclasts that resorb bone. The role of OSM in maintaining normal bone homeostasis has been documented in several *in vitro* and *in vivo* models including OSM and OSMRβ knockout mice that show reduced osteoclast differentiation and activity (27-30). There is also evidence that OSM induces mineralization in mouse osteoblast cells (31); however, during disease states such as osteoarthritis and osteolytic bone metastasis, the balance of OSM and other IL-6/gp130 cytokines has been shown to be severely disrupted, often leading to bone degradation (25).

Breast cancer-derived bone metastasis leads to the dysregulation of IL-6, IL-11, and various growth factors such as receptor activator of NFκB (RANKL), macrophage-colony stimulating factor (MCSF), and VEGF by different cell types including osteoblasts, stromal cells, and immune cells (4, 23, 32, 33). These factors promote osteoclast differentiation and activity, leading to increased bone resorption and compromised structural bone integrity. Currently, there are no published investigations addressing the *in vivo* role of OSM in breast cancer metastasis to bone.

To investigate the effect of OSM on bone metastasis, we utilized the 4T1.2 syngeneic mouse model of breast cancer. The 4T1.2 cell line (34) is a subclone of 4T1 cells that were originally derived from a spontaneous mammary tumor in a Balb/c/C3H mouse (35). When injected orthotopically, 4T1.2 cells metastasize to bone as well as lung, adrenal glands, and lymph nodes (34): a metastatic pattern similar to that seen in breast cancer patients. In this study, we generated modified cell lines by knocking down expression of OSM (4T1.2-OSM) and show that a lack of OSM expression is sufficient to inhibit metastasis to bone from the primary mammary tumor as well as increase survival. Additionally, osteolysis observed after intratibial injection of 4T1.2-OSM cells is significantly reduced in mice compared to control cells. By treating co-cultures of 4T1.2 and RAW 264.7 cells (peripheral blood mononuclear cells (PBMCs), a cellular model of pre-osteoclasts) with OSM, we show that OSM-induced secretion of IL-6, VEGF, and amphiregulin (AREG) promote osteoclastogenesis. Altogether, these findings indicate that targeting OSM expression and signaling provide a novel therapeutic approach for treatment of metastatic breast cancer.

## Results

### OSM increases the invasive potential of mammary tumor cells *in vitro*

Previous results from our group indicate that OSM may play an important role in early stages of metastasis (13, 14, 20). Mouse mammary tumor 4T1.2 cells were characterized *in vitro* to establish them as a credible model for studying OSM signaling *in vivo*. First, we evaluated OSM and OSMRβ expression levels by comparing the highly

metastatic 4T1.2 mammary tumor cells to a non-bone metastatic cell line, 66c14, also derived from the same Balb/c/C3H mammary tumor. 4T1.2 cells secreted 2-fold more OSM and expressed 2.5-fold more OSM receptor (OSMRβ), as compared to 66c14 cells (Fig. 1A and B). The treatment of 4T1.2 cells with OSM (25 ng/ml) resulted in a 20% reduction in adherent cells by day 10 (Fig. 1C, left) and a 60-fold induction of viable tumor cell detachment by day 8 (Fig. 1C, right). The decrease in adherent cell number could be explained by the increase in cell detachment or effects on proliferation.

In addition, we observed an approximate 50% increase in 4T1.2 cell invasive potential after a 24 hour exposure to OSM using a Matrigel invasion assay (Fig. 1D). The above experiments confirmed that OSM signaling is intact in 4T1.2 cells and that these cells can be used to study the contribution of OSM to metastasis to bone *in vivo*.

**OSM is necessary for mammary tumor metastasis to bone**

To examine whether OSM is required for mammary tumor metastasis to bone, we undertook stable knockdown of OSM expression (Fig. 2A; left panel). Three independent OSM shRNA sequences were cloned into the pSilencer4.1 vector, transfected into 4T1.2 mouse mammary tumor cells, and two clonal cell populations showed reduced OSM expression. Of the two clones, 4T1.2-OSM2 cells secreted the lowest levels of OSM (72% less OSM; 14.9 ± 2.3 pg/ml) by ELISA compared to 4T1.2-LacZ control cells (53.1 ± 8.8 pg/ml; Fig. 2A), and 4T1.2-OSM1 cells secreted 30% less OSM (37.0 ± 5.9 pg/ml) (Fig. 2A). OSM mRNA expression levels were confirmed by semi-quantitative RT-PCR (Fig. 2A, inset). To test the effects of OSM on mammary tumor metastasis *in vivo*, control 4T1.2-LacZ, 4T1.2-OSM1, and 4T1.2-OSM2 cells were injected orthotopically into the mammary fat pads of Balb/c mice. As OSM has been shown to have anti-proliferative effects on breast cancer cells *in vitro* (9, 10), we hypothesized that low levels of OSM should result in increased tumor growth *in vivo*. Injection of 4T1.2-OSM2 cells, which displayed the largest decrease in tumor cell-secreted OSM, led to a significant increase in average tumor growth (1,628 $mm^3$ for 4T1.2-OSM2 cells at day 30; Fig. 2B) compared to control 4T1.2-LacZ cells (860 $mm^3$ at day 30; Fig. 2B) and parental 4T1.2 cells (870 $mm^3$ at day 30; data not shown). Injection of 4T1.2-OSM1 cells, which displayed a modest decrease in tumor cell-secreted OSM, resulted in tumor growth similar to control cells (861 $mm^3$ at day 30; Fig. 2B).

Metastasis to bone in mice injected with control 4T1.2-LacZ, 4T1.2-OSM1, and 4T1.2-OSM2 cells was quantified by qPCR, which measures the amount of vector DNA contained in all three cell types. Mean bone metastatic burden in spine was significantly lower in mice that received 4T1.2-OSM1 or 4T1.2-OSM2 cells, compared to 4T1.2-LacZ control cells (Fig. 2C). Histological evaluation of vertebrae by H & E staining revealed the presence of metastatic tumor cells in the bone marrow of mice injected with 4T1.2-LacZ control cells but not in the bone marrow of mice injected with 4T1.2-OSM2 cells (Fig. 2D). After careful inspection, a small intraosseous metastasis was identified in vertebrae from a mouse injected with 4T1.2-OSM1 cells, explainable by the fact that these cells did not demonstrate as robust an OSM expression knockdown as the 4T1.2-OSM2 cells. Overall, these results suggest that tumor cell-expressed OSM is necessary for mammary tumor metastasis to bone.

In addition to the increased tumor growth and decreased metastasis to bone observed in mice injected with 4T1.2-OSM2 cells *in vivo*, these cells also demonstrate decreased invasive potential *in vitro*. Specifically, 4T1.2-OSM2 cells displayed an increase in adherent cell number over time (data not shown), a decrease in viable cell detachment (Supplemental Fig 1A), and a decrease in invasive potential (Supplemental Fig 1B) compared to 4T1.2-LacZ control cells. These results demonstrate that 4T1.2-OSM2 cells display a reduced invasiveness *in vitro* and provide an appropriate model for subsequent *in vivo* experiments.

**OSM promotes mammary tumor cell-mediated osteolysis *in vivo***

4T1.2-OSM2 and control cells were injected into the tibia of Balb/c mice. Legs excised four weeks after injection of control 4T1.2-LacZ cells showed significant osteolysis in the proximal end of the tibia, as analyzed by Micro CT. The same region in mice injected with 4T1.2-OSM2 cells showed less osteolysis, more closely resembling PBS-injected animals (Fig. 3A); however, a mixed osteolytic/osteoblastic phenotype was seen. Analysis of trabecular bone revealed extensive osteolysis due to 4T1.2-LacZ cells, prohibiting 3D reconstruction of the region of interest (ROI) in all but one animal (Fig. 3B, top and Supplemental Fig. 2A). Mice injected with 4T1.2-OSM2 cells displayed a trabecular bone morphology more similar to that of PBS-injected mice (Fig. 3C, top and Supplemental Fig. 2A). A similar pattern was observed in the cortical bone (Fig. 3B, bottom and Supplemental Fig. 2B).

Quantitative analysis of trabecular and cortical bone was performed using ROIs (50 x 10 μm slices). Mice injected with 4T1.2-OSM2 cells displayed a dramatically greater total trabecular bone volume and trabecular thickness when compared to control 4T1.2-LacZ cells (Fig. 3C). Both cortical bone volume/total volume and cortical bone mineral density were significantly higher in 4T1.2-OSM2 cell-injected mice as compared to mice injected with control cells (Fig. 3C). Overall, these quantitative results indicate that OSM expression is important for osteolytic activity of 4T1.2 cells in the bone microenvironment.

**Lack of mammary tumor cell-derived OSM increases survival *in vivo***

To determine the influence of decreased OSM expression on bone metastasis independent of its effects on primary tumor growth, we utilized a tumor resection model. Orthotopic mammary fat pad injections were performed using control 4T1.2-LacZ and 4T1.2-OSM2 cells, primary tumors were resected at day 14 (Fig. 4A), and mice were monitored until endpoint criteria were met (see Materials and Methods). The survival time for mice that received 4T1.2-OSM2 cell injections significantly increased by a mean of 10 days and a maximum of 42 days compared to control 4T1.2-LacZ cells (Fig. 4B). In addition, mice injected with 4T1.2-OSM2 cells had no detectable metastases in the spines, as analyzed by qPCR, whereas all of the mice injected with 4T1.2-LacZ cells demonstrated high levels of metastases in the spine (Fig. 4C). Lung metastases were detectable in both the 4T1.2-LacZ and 4T1.2-OSM2 groups of mice at the time of sacrifice; however, the time for maximum metastasis to the lungs was significantly delayed in the 4T1.2-OSM2 injected group (data not shown). These results indicate that following primary tumor resection, decreased OSM expression in mammary tumor cells delayed bone metastasis and increased the animal survival rate.

**OSM induces tumor cell-mediated osteoclastogenesis**

To identify the mechanism by which mammary tumor cell-derived OSM causes osteolysis, an *in vitro* model of osteoclastogenesis mimicking PBMC-derived osteoclasts was employed using RAW 264.7 mouse monocytic cells co-cultured with 4T1.2 cells. The capacity of each cell type to respond to OSM and other OSM-related factors was analyzed by semi-quantitative RT-PCR. Both the RAW 264.7 cells, which are able to undergo osteoclast differentiation, and the 4T1.2 mouse mammary tumor cells expressed the gp130 subunit necessary for all IL-6 family receptors (Fig. 5A). 4T1.2 cells expressed OSMRβ, LIFRβ, and IL-6R, while RAW 264.7 cells expressed IL-6R and barely detectable levels of LIFRβ (Fig. 5A). Therefore, in our *in vitro* model of osteoclastogenesis, we predicted that the 4T1.2 cells should respond to OSM, LIF, and IL-6 and that the RAW 264.7 cells should not respond to OSM.

The ability of 4T1.2 cells to induce osteoclastogenesis in response to OSM was assessed. A 7.5-fold increase in TRAP-positive (TRAP+) cells, a marker of osteoclast differentiation, was observed in OSM-treated RAW 264.7 and 4T1.2 co-cultures compared to untreated co-cultures in the presence of 5ng/mL MCSF and 10 ng RANKL (Fig. 5B). To demonstrate the importance of OSM-mediated secreted factors from 4T1.2 cells, conditioned medium (CM) was collected from 4T1.2 cells treated with or without OSM and applied to RAW 264.7 cells. An approximate 3-fold increase in TRAP+ osteoclasts was observed in RAW 264.7 cells cultured with CM (+OSM) compared to CM (-OSM) (Fig. 5B). No significant difference in the level of osteoclastogenesis was observed when RAW 264.7 cells alone were treated with OSM (Fig. 5B.)

**Mammary tumor cells secrete pro-osteoclastogenic factors in response to OSM**

To identify which 4T1.2 cell-secreted pro-osteoclastogenic factors were increased in response to OSM, ELISA and Western blot analyses were performed. No difference in the levels of 4T1.2 cell-derived RANKL, MCSF, transforming growth factor beta (TGFβ), or tumor necrosis factor alpha (TNFα) was observed after treatment with OSM (Supplemental Table 2). However, levels of IL-6 and VEGF, whose receptors are both present on RAW 264.7 cells (Fig. 5A), were significantly increased in response to OSM (Fig. 5C and D). 4T1.2 cells alone, as well as RAW 264.7 and 4T1.2 cell co-cultures showed a 3- to 4-fold increase in secreted IL-6 levels when treated with OSM (Fig. 5C). RAW 264.7 cells alone did not show a significant increase in IL-6 in response to OSM (Fig. 5C). VEGF secretion by 4T1.2 cells was increased 2-fold following treatment with OSM verses untreated cells (Fig. 5D). Secreted VEGF levels increased 7-fold in treated co-cultures compared to untreated 4T1.2 cells, suggesting that in addition to OSM treatment, a direct interaction between the two cell types may cause an increase in VEGF.

**OSM-induced amphiregulin in mammary tumor cells increases osteoclastogenesis**

Amphiregulin (AREG), a member of the epidermal growth factor (EGF) family and previously unknown to be induced by OSM, was identified by proteome array analysis (R&D Systems) of conditioned medium from 4T1.2 cells treated with OSM (see Supplemental Materials and Methods). A more than 2-fold increase in secreted AREG was verified by ELISA in CM collected from OSM-treated 4T1.2 cells as compared to untreated cells (Fig. 6A, left). Co-culturing RAW 264.7 cells with 4T1.2 cells had no effect on OSM-induced AREG secretion levels, and RAW 264.7 cells alone did not increase AREG secretion in response to OSM (Fig. 6A, left). To determine whether AREG plays a direct role in osteoclastogenesis in our *in vitro* model, recombinant AREG (50 ng/ml) was added to co-cultures of RAW 264.7 and 4T1.2 cells in the presence of 5 ng/mL MCSF and 10 ng RANKL. AREG supplementation increased the number of TRAP+ osteoclasts by 2-fold in these co-cultures, and addition of OSM with AREG further increased the number of TRAP+ osteoclasts by nearly 9-fold compared to untreated controls (Fig. 6A, right). AREG showed a minimal effect on osteoclastogenesis in cultures of RAW 264.7 cells alone (Fig. 6A, right). Inhibition of AREG signaling using a neutralizing antibody in RAW 264.7 and 4T1.2 cell co-cultures resulted in a near complete suppression of OSM-mediated osteoclastogenesis (Fig. 6B, left). No significant effect was seen in RAW 264.7 cultures (Fig. 6B, left). A combination of anti-IL-6, anti-VEGF, and anti-AREG antibodies did not significantly reduce osteoclastogenesis beyond co-cultures treated with anti-AREG only (Fig. 6B, right). Anti-IL-6 or anti-VEGF antibodies alone had less effect on inhibition of OSM-induced osteoclastogenesis in co-cultures than anti-AREG (Fig. 6B, right). Thus, OSM-induced AREG appears to be a key player in mammary tumor cell-induced osteoclastogenesis *in vitro*.

**OSM inhibits osteoprotegrin expression in tumor cells**

Osteoprotegrin (OPG), the decoy receptor for RANKL, is an important endogenous inhibitor of osteoclastogenesis. Preliminary data from our group have shown expression of OPG is decreased by RT-PCR in a panel of human breast cancer cells treated with OSM (data not shown). Therefore, we investigated the effect of OSM on OPG expression by 4T1.2 mouse mammary tumor cells by both RT-PCR and ELISA. OSM treatment of 4T1.2 cells resulted in a 40% reduction in secreted OPG levels by ELISA (Fig. 6C; left) and an 80% reduction in mRNA expression by RT-PCR (Fig. 6C; right). Interestingly, the addition of recombinant AREG (25 ng/ml) also resulted in an 80% decrease in OPG expression (Fig. 6C; right), suggesting that OSM-mediated osteoclastogenesis may act through AREG suppression of OPG.

## Discussion

This study provides evidence that tumor cell-secreted OSM promotes osteolytic breast cancer metastasis to bone. Our data indicate that OSM is important in late stages of the metastatic process but may also be necessary for earlier stages. We show, specifically: i) OSM induces 4T1.2 mouse mammary tumor cell detachment and invasion *in vitro*; ii) mice orthtopically injected with 4T1.2 tumor cells with reduced OSM expression exhibit decreased bone metastases and increased survival; iii) intratibial injections of the above 4T1.2 cells in mice result in decreased osteolysis; and iv) a novel mechanism for OSM promoting tumor cell-secreted amphiregulin during osteoclast differentiation was identified.

The syngeneic 4T1.2 mouse model is the only reliable model for spontaneous mammary tumor metastasis to bone currently available. Intracardiac or intratibial injections of osteolytic human breast cancer cells into immunocompromised athymic mice to study the role of OSM in bone metastasis is problematic due to a lack of homology between human and mouse OSM signaling (36), as well as the need for intact immune function to adequately study the effect of an inflammatory cytokine on metastasis. Using our 4T1.2-OSM2 orthotopic mouse model, we observed a dramatic decrease in bone metastasis despite increased tumor growth. A dual role as an anti-proliferative and yet pro-metastatic factor in breast cancer metastasis has been shown with other breast cancer cell secreted factors such as transforming growth factor beta (TGFβ). TGFβ is not regulated by OSM in 4T1.2 cells (Supplemental Table 2) but is known to increase invasion and metastasis of breast tumors along with its tumor cell growth inhibitory effects (37). To date, this is the first study demonstrating an independent and yet similar role for OSM driving breast cancer metastasis to bone, despite inhibitory effects on primary tumor growth.

Bone is the most common site of metastatic disease in breast cancer patients (1), although metastasis also occurs to lung, liver, adrenal glands, brain, kidney, spleen, heart, and lymph nodes. Specific quantification of metastatic burden by qPCR was conducted for spine and lung only (Fig. 2C; data not shown) and both were significantly reduced in mice orthotopically injected with 4T1.2-OSM1 and 4T1.2-OSM2 cells. By utilizing a tumor resection model, we were able to increase the time it took to reach overall maximum metastatic burden and identify other important metastatic sites modulated by OSM. Upon dissection of these mice at maximum metastatic endpoint, sites with visual metastases, in addition to the spine, were lung, liver, and lymph nodes. A reduction in the number of lung metastases or prolongation of the time to lung metastasis development may explain the significant increase in survival seen in mice that had resected primary tumors with reduced OSM expression. Therefore, the lung was identified as another major metastatic site affected by OSM and is being investigated further. Overall, OSM is likely critical for both late as well as early stages of metastasis, resulting in an increase in total metastatic burden. However, our data suggest a more significant role for OSM during later steps of the metastatic process, specifically in the bone microenvironment.

4T1.2-OSM2 tumor cells injected directly into the bone microenvironment of the tibia revealed that tumoral OSM expression is critical for induction of osteolysis in both trabecular and cortical bone. In general, 4T1.2-OSM2 cell-injected mice showed a mixed osteolytic/osteoblastic phenotype, similar to what is seen in human metastatic breast cancer patients (38). Previous studies analyzing intrafemoral injection of 4T1 cells (the parental cells for the 4T1.2 subclone used in this manuscript) show only osteolytic activity by Micro CT (39). This manuscript is the first study presenting Micro CT data from intratibial injections of the 4T1.2 subclone. 4T1.2 cells injected into the mouse tibia resulted in some osteoblast activity, although overall the osteolytic phenotype was predominant (see Supplemental Figure 2). OSM has been shown previously to play a dual role in the normal bone microenvironment stimulating both bone resorption as well as bone formation. Specifically, OSM has been shown to promote osteoclastogenesis and osteoclast activity by STAT3-induced RANKL expression in osteoblast/stromal cells (40) yet will stimulate osteogenesis in mesenchymal stem cells and mineralization in murine osteoblast cells (31, 40). The role of OSM in osteoblastogenesis and mineralization in our breast cancer metastasis model is currently being conducted. However, we have measured osteoclast activity *in vitro* using a synthetic bone resorption assay, and increased bone resorption was detected using a mixed population of mouse primary pre-osteoclasts and pre-osteoblasts cultured in CM from 4T1.2 cells treated with OSM (data not shown). Increased osteolysis in the animals injected with 4T1.2-LacZ cells compared to parental 4T1.2 cells was also noted (see Supplementary Figure 2). siRNA/shRNA technology has been shown to cause generally unavoidable off-target effects related to immune system activation, as the siRNA machinery is physiologically associated with viral infections (41, 42) that can potentially lead to aberrant osteoclastogenesis and osteolysis. Overall, our studies suggest that tumor cell-derived OSM leads to an increase in both osteoclast differentiation and activity that result in osteolytic bone lesions.

Using an *in vitro* co-culture system of osteoclast differentiation, this work presents evidence for several OSM-induced tumor secreted factors that could mediate the observed *in vivo* osteolysis. The RAW 264.7 mouse monocytic cell line was chosen as a source of pre-osteoclast cells in our *in vitro* model of tumor cell/bone microenvironment interaction instead of bone marrow cells derived from Balb/c mice. This decision was based on recent studies suggesting that peripheral blood mononuclear cells (PBMCs) that include monocytes, are a major source of osteoclasts in pathologic osteolysis. PBMCs isolated from patients with bone metastases have been shown to undergo spontaneous osteoclastogenesis (43-45), while similar effects with bone marrow cells isolated from cancer patients have not been reported. Furthermore, we were able to maximize OSM-induced effects on osteoclastogenesis in our co-culture system by the addition of very low levels of RANKL and MCSF to all the assays. The low level of these key osteoclast-promoting factors resulted in the formation of predominantly mononuclear TRAP+ cells, which, nonetheless, had direct osteolytic activity (data not shown; (46)). The significant increase in RAW 264.7 TRAP+ cells in OSM-treated co-cultures with 4T1.2 cells or conditioned media from 4T1.2 cells treated with OSM was mediated in part by IL-6 and VEGF. Both IL-6 and VEGF have been shown by our group and others to promote osteoclast differentiation and activity (47, 48), and VEGF expression has been detected in osteolytic bone metastases (49). To identify novel OSM-induced factors, a proteome array analysis of conditioned medium from 4T1.2 cells treated with OSM was performed, and AREG was identified. AREG is membrane-bound until cleaved by the protease ADAMTS1 (a disintegrin and metalloproteinase with thrombospondin motifs 1), expression of which was also induced by OSM in 4T1.2 cells (Supplemental Table 2). AREG has been associated with several mechanisms of breast cancer progression including tumor cell proliferation and the expression of proteases such as MMP2 and MMP9 (50) and is expressed at moderate to high levels in human infiltrating breast carcinoma (51, 52).

The role of AREG in breast cancer metastasis to bone has not been studied extensively. AREG has been shown to increase expression of parathyroid hormone related protein (PTHrP) from breast cancer cells *in vitro*, however in studies of human breast cancer bone metastases, it is unclear as to whether PTHrP expression drives the metastasis to bone or the bone microenvironment induces PTHrP expression (53). In our 4T1.2 co-culture model, OSM-induced AREG did not promote expression or secretion of PTHrP by RT-PCR and ELISA (Supplemental Table 2), but instead, resulted in decreased secretion of the decoy receptor for RANKL, osteoprotegrin (OPG). This is the first time AREG and OSM have been shown to decrease OPG secretion from tumor cells, although a previous study demonstrated that AREG inhibits OPG secretion by osteoblasts, the primary source of this factor (54). AREG is known to bind to the epidermal growth factor receptor (EGFR or ErbB1) for downstream signaling; however, a recent publication and our Western blot analysis indicate that 4T1.2 cells do not express this receptor (55). With 4T1.2 cells, it is possible that AREG binds an alternative receptor such as ErbB3/HER3 (56) to inhibit OPG expression. OPG is associated with decreased osteoclastogenesis, and increased OPG expression in breast cancer cells has been shown to protect against osteolytic tumor growth in bone (57). A proposed model summarizing our *in vitro* results is illustrated in Figure 7, in which OSM induces VEGF, IL-6, and AREG secretion from breast tumor cells. Secreted VEGF and IL-6 bind to pre-osteoclasts to promote osteoclast differentiation, while AREG signals tumor cells to inhibit the production of the anti-osteoclastic factor OPG.

In conclusion, this study demonstrates that tumor cell-derived OSM promotes osteolytic bone metastasis. We propose this may be through a novel OSM-induced tumor-secreted factor AREG that leads to an increase in osteoclast activation by suppressing OPG. Current therapies for osteolytic bone metastases, such as bisphosphonates, alleviate patient symptoms but have limited effect on inhibiting tumor cell metastasis to bone and relevant specific breast tumor-derived factors responsible for osteolysis. Based on this study, we suggest that OSM could be a viable therapeutic target for patients with surgically removed primary tumors to reduce bone metastasis and prevent bone loss.

## Materials and Methods

### Cell lines and culture conditions

66c14 and 4T1.2 cells were maintained in DMEM media supplemented with 10% fetal bovine serum (FBS), 1 mM sodium pyruvate, and 100 units/ml each of penicillin and streptomycin. RAW 264.7 cells were obtained directly from the American Type Culture Collection (Rockville, MD), cultured in MEMα media with the same supplements, and passaged for no more than 6 months. Cells were maintained at 37 $^{o}$C, 5% carbon dioxide, and 95% humidity. All media and supplements were obtained from Hyclone (Logan, UT). 66c14 and 4T1.2 mouse mammary cell lines were generated by the authors; therefore, there are no external lines against which they can be authenticated.

### Adherent Cell Count/Proliferation, Detachment, and Invasion Assays

To assess the number of viable adherent cells correlating with proliferation, 1.0 x $10^3$ cells were seeded in 24-well plates with 1 ml of complete medium and treated with or without 25 ng/mL recombinant mouse OSM (R&D systems, Minneapolis, MN). Cells were detached using 0.25% trypsin (Hyclone) and counted using a hemocytometer every 2 days. OSM-stimulated tumor cell detachment and invasion were conducted as described previously (20) with the following modifications to the invasion assay. A total of 2.5 x $10^4$ cells were plated with or without 25 ng/mL OSM in the upper chamber of the Matrigel-coated invasion chambers (BD Biosciences, Bedford, MA) in normal growth medium without serum, and normal growth medium containing 10% FBS was added to the bottom chamber as a chemoattractant. Staining of the invasion chambers was achieved with 0.05% crystal violet. Each Matrigel-coated or uncoated control membrane was counted in its entirety for each experiment. Data for invasion assays is presented % invasion (# of cells that migrated through Matrigel-coated membranes/ # of cells that migrated through control membranes), according to manufacturer's instructions.

### Enzyme Linked Immunosorbent Assay (ELISA)

To measure OSM, AREG, and OPG in conditioned medium, a direct or sandwich ELISA was developed (see Supplemental Materials and Methods). For the measurement of mouse VEGFA and mouse IL-6 in conditioned medium, ELISA kits (R&D systems) were utilized according to manufacturer's instructions. For all ELISAs, 1 x

$10^5$ cells were plated per well in a 24-well plate in serum-free media and conditioned medium was collected 48 hours later.

**Reverse-transcriptase PCR (RT-PCR)**

To determine the relative expression of various receptors in 4T1.2 and RAW 264.7 cells, RNA was extracted from these cells using RNA-STAT60 (Teltest, Friendswood, TX) according to manufacturer's instructions, and RNA integrity was assessed using the bleach gel method as recently described (58). cDNA was synthesized using GeneAmp RNA PCR kit (Applied Biosystems Carlsbad, CA) and amplified using the GoTaq PCR kit (Promega, Madison, WI). Primer sequences and annealing temperatures ($T_A$) are listed in Supplemental Table 1. The thermocycler conditions for all PCR reactions were as follows: 95°C for 2 min, 29 cycles of 95°C for 1 min, $T_A$ for 30 seconds, and 72 °C for 1 min and 72 °C for 1 min after the 29 cycles. Relative amount of RNA was quantified by densitometry of PCR products run on 0.5% agarose gels containing ethidium bromide.

**Plasmid construct design and cell transfections.**

To create OSM knockdown vectors, OSM
shRNA sequences were cloned into the pSilencer 4.1 plasmid (Ambion, Austin, TX). A total of three shRNA constructs (1-3) were tested for OSM knockdown as well as a LacZ control using the same loop sequence of TTCAAGAGA and the following sense(s) and antisense(a) sequences: OSM1s-GGACAGAGTCTTGTACCAACT, OSM1a- AGTTGGTACAAGACTCTGTCC; OSM2s-GTACCAACTGGATGCTTTA, OSM2a-TAAAGCATCCAGTTGGTACAA; OSM3s-GCACAATATCCTCGGCATAAG, OSM3a-CTTATGCCGAGGATATTGTGC; LacZs-GCTCCAAAGAAGAAGCGTT; LacZa-AACGCTTCTTCTTTGGAGC. 4T1.2 cells were transfected with the pSilencer 4.1 constructs containing the various mOSM shRNAs using lipofectamine LTX (Invitrogen Carlsbad, CA) reagent, as per manufacturer instructions. Stably transfected cell lines were grown in the presence of 0.3 mg/mL of the neomycin analogue G418 (Sigma Aldrich). All established cell lines were checked for OSM expression by ELISA.

**Animals and Tumor Cell Injections**

Six-week-old female Balb/c mice were obtained from the National Cancer Institute's Animal Production Facility (Frederick, MD). For orthotopic injections, each mouse was anesthetized by i.p. injection of 6.25 mg/kg of sodium pentobarbital or with 2.5% isoflurane and $1.0x10^5$ cells diluted in 10 μL of PBS containing 10% medium were injected into the 4th mammary fat pad. For intratibial injections, $1 \times 10^4$ cells in 30 μl PBS containing 10% medium were injected and needle placement was verified by X-ray as previously described (59). For tumor resection, mammary tumors were surgically excised 14 days after orthotopic injections. All animal studies were conducted in accordance with the protocol approved by the Institutional Animal Care and Use Committee (IACUC) at the Boise VA Medical Center, Washington University School of Medicine in St. Louis, MO, or the Peter MacCallum Cancer Centre in Melbourne, Australia. Starting at 2 weeks post-injection, tumor length and width were measured by mechanical calipers 3 times a week and tumor volume was extrapolated using the following equation (tumor volume = (length x width$^2$) /2). "Survival endpoint" was defined by the IACUC as tumor size greater than 20 mm in diameter, 10% or more weight loss, and/or appearance of cachexia.

**Quantitative PCR (qPCR)**

Spines dissected from mice bearing mammary tumors were stripped of any soft tissue, snap-frozen in liquid nitrogen, and pulverized into a fine powder. DNA was extracted using an STE buffer containing 20 μl/ml of proteinase K and purified by two phenol/chloroform (1:1 v/v) extractions followed by ethanol precipitation. The ratio of cancer cells to normal cells was quantified by measuring genomic DNA levels for the neomycin resistance gene ($neo^r$) found integrated in tumor cells versus the DNA levels for a control gene vimentin present in all cells, as described previously (60). Taqman PCR was performed on an Applied Biosystems 7500 real-time thermocycler. Probe and primer sequences are listed in Supplemental Table 1. The cycling conditions were run as follows: 50 °C for 5 minutes, 95 °C for 2 minutes, then 40 cycles of 95 °C for 1 minutes and 60 °C for 45 seconds. Fluorescence was measured every cycle after the annealing step and threshold cycle number ($C_t$) values were calculated. The data was analyzed using the comparative $\Delta C_t$ method (61).

### Histology

To verify the location of spine metastasis, spines from each experimental group (4T1.2-LacZ, n=2; 4T1.2-OSM2, n=2; and 4T1.2-OSM1, n=1) were placed in ultralight fixative (Ultralight Histology, Nampa, ID) paraffin embedded, and sectioned (Bi-Biomics, Nampa, ID). For each spine, four 1 μm sections were collected 10 μm apart in the lumbar region and H&E stained.

### Micro-computed tomography (Micro CT) Analysis of *In Vivo* Osteolysis

For determining the 3-D architecture of the trabecular and cortical bone, mice were euthanized and the hind limb was removed and placed in 10% formalin overnight before being transferred to 70% ethanol for analysis using a vivaCT40 scanner (Scanco Medical AG, Switzerland). Tube settings were at 55 kVp and 145 μA with a tube diameter of 21.5 mm. The entire hind limb (femur, tibia, and fibula) was scanned at a 10 μm isometric resolution with 250 ms integration time. For trabecular bone analysis, the end of the growth plate was used as the landmark and a 0.525 mm (50 slices) region below the landmark (metaphysis) was considered as the region of interest (ROI). Contours were drawn on 50 slices distal to the landmark around the trabecular bone only (endo-cortical boundary). An additional analysis of the cortical bone below the growth plate was performed from the trabecular bone analysis scans. The mid-diaphyseal region (approximate middle of the proximal-end and tibia-fibula junction) of the tibia was considered as the ROI for cortical bone analysis. Two contours were drawn on 50 slices of the ROI; one at the periosteal surface (inclusive) including the cortical bone and other at the endosteal surface of the bone (exclusive) to exclude the medullary region. A Gaussian filter (with Gaussian sigma of 0.4, and Support of 1) was applied on all slices before image segmentation. All the contoured slices were segmented and analyzed with the global threshold value of 250 'per-mille' (Linear attenuation coefficient (μ) of 2.00 [1/cm]).

### Osteoclastogenesis Assay

$1.0 \times 10^4$ RAW 264.7 cells were added to each well of a 24-well plate in duplicate in complete MEMα medium containing 50mg/L L-ascorbic acid. $1.0 \times 10^3$ 4T1.2 cells were plated in co-culture with the RAW 264.7 cells or alone and 25 ng/ml OSM and/or 50 ng/ml AREG were added. All osteoclastogenesis assays included very low levels of RANKL and MCSF (10 ng/ml RANKL and 5 ng/ml of MCSF). Two hours before the addition of OSM, AREG, VEGF, and IL-6 neutralizing antibodies were added at final concentration of 1 μg/ml where indicated. All mouse factors and antibodies were obtained from R&D Systems Minneapolis, MN. The co-cultures were maintained for 9-10 days without any changes of the medium and osteoclasts were stained using a tartrate resistant acid phosphate (TRAP) stain kit (Sigma Aldrich St. Louis, MO) according to manufacturer's instructions. TRAP-positive cells that stained purple were counted and quantified per well.

### Statistical Analysis

Data are displayed as mean ± standard error of the mean (SEM). Data were analyzed using an unpaired student's t-test or analysis of variance (ANOVA) with Tukey's multiple comparison post-hoc test where appropriate, using Prism GraphPad 5.0b software (GraphPad Software Inc., San Diego, CA). Survival data were analyzed using the Log-rank (Mantel-Cox) test. Asterisks denote *$p<0.05$, **$p<0.01$, or ***$p<0.001$.

## Conflict of Interest

The authors declare no potential conflicts of interest with respect to the authorship and/or publication of this article.

## Acknowledgements

Special thanks is given to John Englebach, Joel Garbow, and Tarpit Patel for assistance with Micro CT experiments, Dr. Dondelinger and Tyson Nielson (Bi-Biomics Inc., Nampa, ID) for assistance with H & E and pathology, and Christina Restall (Peter MacCallum Cancer Centre, Melbourne, Australia) for assistance with the orthotopic mouse model and qPCR.

**Funding**

This work was supported by the American Cancer Society [ACS RSG-09-276-01-CSM]; Susan G Komen for the Cure [KG100513]; National Institutes of Health [NIH/NCRR P20RR016454]; National Aeronautics and Space Administration [NASA NNX10AN29A]; and the National Breast Cancer Foundation (NBC, Australia) (RLA). Mice were maintained at the VA Medical Center, Boise, ID, which is supported in part by the National Institutes of Health [NIH/NIAMS P30AR057235].

## References

1. Jemal A, Siegel R, Xu J, Ward E. Cancer statistics, 2010. CA: a cancer journal for clinicians. 2010;60(5):277-300.
2. Coleman RE. Skeletal complications of malignancy. Cancer. 1997;80(8 Suppl):1588-94.
3. Tumminello FM, Badalamenti G, Incorvaia L, Fulfaro F, D'Amico C, Leto G. Serum interleukin-6 in patients with metastatic bone disease: correlation with cystatin C. Medical oncology (Northwood, London, England). 2008.
4. Heinrich PC, Behrmann I, Haan S, Hermanns HM, Muller-Newen G, Schaper F. Principles of interleukin (IL)-6-type cytokine signalling and its regulation. The Biochemical journal. 2003;374(Pt 1):1-20.
5. Korzus E, Nagase H, Rydell R, Travis J. The mitogen-activated protein kinase and JAK-STAT signaling pathways are required for an oncostatin M-responsive element-mediated activation of matrix metalloproteinase 1 gene expression. J Biol Chem. 1997;272(2):1188-96.
6. Liu J, Hadjokas N, Mosley B, Estrov Z, Spence MJ, Vestal RE. Oncostatin M-specific receptor expression and function in regulating cell proliferation of normal and malignant mammary epithelial cells. Cytokine. 1998;10(4):295-302.
7. Hurst SM, McLoughlin RM, Monslow J, Owens S, Morgan L, Fuller GM, et al. Secretion of oncostatin M by infiltrating neutrophils: regulation of IL-6 and chemokine expression in human mesothelial cells. J Immunol. 2002;169(9):5244-51.
8. Badache A, Hynes NE. Interleukin 6 inhibits proliferation and, in cooperation with an epidermal growth factor receptor autocrine loop, increases migration of T47D breast cancer cells. Cancer Res. 2001;61(1):383-91.
9. Liu J, Spence MJ, Wallace PM, Forcier K, Hellstrom I, Vestal RE. Oncostatin M-specific receptor mediates inhibition of breast cancer cell growth and down-regulation of the c-myc proto-oncogene. Cell Growth Differ. 1997;8(6):667-76.
10. Horn D, Fitzpatrick WC, Gompper PT, Ochs V, Bolton-Hansen M, Zarling J, et al. Regulation of cell growth by recombinant oncostatin M. Growth factors (Chur, Switzerland). 1990;2(2-3):157-65.
11. Mori S, Murakami-Mori K, Bonavida A. Oncostatin M (OM) promotes the growth of DU 145 human prostate cancer cells, but not PC-3 or LNCaP, through the signaling of the OM specific receptor. Anticancer Research. 1999;19(2A):1011-5.
12. Li QH, Zhu JH, Sun F, Liu L, Liu XX, Yue Y. Oncostatin M promotes proliferation of ovarian cancer cells through signal transducer and activator of transcription 3. International Journal of Molecular Medicine. 2011;28(1):101-8.
13. Holzer RG, Ryan RE, Tommack M, Schlekeway E, Jorcyk CL. Oncostatin M stimulates the detachment of a reservoir of invasive mammary carcinoma cells: role of cyclooxygenase-2. Clin Exp Metastasis. 2004;21(2):167-76.
14. Jorcyk CL, Holzer RG, Ryan RE. Oncostatin M induces cell detachment and enhances the metastatic capacity of T-47D human breast carcinoma cells. Cytokine. 2006;33(6):323-36.
15. Argast GM, Mercado P, Mulford IJ, O'Connor M, Keane DM, Shaaban S, et al. Cooperative signaling between oncostatin M, hepatocyte growth factor and transforming growth factor-beta enhances epithelial to mesenchymal transition in lung and pancreatic tumor models. Cells, tissues, organs. 2010;193(1-2):114-32.
16. Hui W, Rowan AD, Richards CD, Cawston TE. Oncostatin M in combination with tumor necrosis factor alpha induces cartilage damage and matrix metalloproteinase expression in vitro and in vivo. Arthritis and rheumatism. 2003;48(12):3404-18.
17. Fossey SL, Bear MD, Kisseberth WC, Pennell M, London CA. Oncostatin M promotes STAT3 activation, VEGF production, and invasion in osteosarcoma cell lines. BMC cancer. 2011;11:125.
18. Soldi R, Graziani A, Benelli R, Ghigo D, Bosia A, Albini A, et al. Oncostatin M activates phosphatidylinositol-3-kinase in Kaposi's sarcoma cells. Oncogene. 1994;9(8):2253-60.
19. Crichton MB, Nichols JE, Zhao Y, Bulun SE, Simpson ER. Expression of transcripts of interleukin-6 and related cytokines by human breast tumors, breast cancer cells, and adipose stromal cells. Molecular and cellular endocrinology. 1996;118(1-2):215-20.
20. Queen MM, Ryan RE, Holzer RG, Keller-Peck CR, Jorcyk CL. Breast cancer cells stimulate neutrophils to produce oncostatin M: Potential implications for tumor progression. Cancer Research. 2005;65(19):8896-904.
21. Celis JE, Gromov P, Cabezon T, Moreira JMA, Ambartsumian N, Sandelin K, et al. Proteomic characterization of the interstitial fluid perfusing the breast tumor microenvironment: a novel resource for biomarker and therapeutic target discovery. Faseb Journal. 2004;18(8):C306-C.

22. Levano KS, Jung EH, Kenny PA. Breast cancer subtypes express distinct receptor repertoires for tumor-associated macrophage derived cytokines. Biochem Biophys Res Commun. 2011;411(1):107-10.
23. Ooi LL, Zheng Y, Stalgis-Bilinski K, Dunstan CR. The bone remodeling environment is a factor in breast cancer bone metastasis. Bone. 2010.
24. Palmqvist P, Persson E, Conaway HH, Lerner UH. IL-6, leukemia inhibitory factor, and oncostatin M stimulate bone resorption and regulate the expression of receptor activator of NF-kappa B ligand, osteoprotegerin, and receptor activator of NF-kappa B in mouse calvariae. J Immunol. 2002;169(6):3353-62.
25. Sims NA, Walsh NC. GP130 cytokines and bone remodelling in health and disease. BMB reports. 2010;43(8):513-23.
26. Song HY, Jeon ES, Kim JI, Jung JS, Kim JH. Oncostatin M promotes osteogenesis and suppresses adipogenic differentiation of human adipose tissue-derived mesenchymal stem cells. Journal of cellular biochemistry. 2007;101(5):1238-51.
27. Minehata K, Takeuchi M, Hirabayashi Y, Inoue T, Donovan PJ, Tanaka M, et al. Oncostatin m maintains the hematopoietic microenvironment and retains hematopoietic progenitors in the bone marrow. International journal of hematology. 2006;84(4):319-27.
28. Tanaka M, Hirabayashi Y, Sekiguchi T, Inoue T, Katsuki M, Miyajima A. Targeted disruption of oncostatin M receptor results in altered hematopoiesis. Blood. 2003;102(9):3154-62.
29. O'Connor JC, Farach-Carson MC, Schneider CJ, Carson DD. Coculture with prostate cancer cells alters endoglin expression and attenuates transforming growth factor-beta signaling in reactive bone marrow stromal cells. Mol Cancer Res. 2007;5(6):585-603.
30. Knowles HJ, Athanasou NA. Hypoxia-inducible factor is expressed in giant cell tumour of bone and mediates paracrine effects of hypoxia on monocyte-osteoclast differentiation via induction of VEGF. J Pathol. 2008;215(1):56-66.
31. Walker EC, McGregor NE, Poulton IJ, Solano M, Pompolo S, Fernandes TJ, et al. Oncostatin M promotes bone formation independently of resorption when signaling through leukemia inhibitory factor receptor in mice. J Clin Invest. 2010;120(2):582-92.
32. Sloan EK, Anderson RL. Genes involved in breast cancer metastasis to bone. Cell Mol Life Sci. 2002;59(9):1491-502.
33. Rose AA, Siegel PM. Breast cancer-derived factors facilitate osteolytic bone metastasis. Bulletin du cancer. 2006;93(9):931-43.
34. Lelekakis M, Moseley J, Martin T, Hards D, Williams E, Ho P, et al. A novel orthotopic model of breast cancer metastasis to bone. Clinical & Experimental Metastasis. 1999:163-70.
35. Aslakson CJ, Miller FR. Selective events in the metastatic process defined by analysis of the sequential dissemination of subpopulations of a mouse mammary tumor. Cancer Res. 1992;52(6):1399-405.
36. Grant SL, Begley CG. The oncostatin M signalling pathway: reversing the neoplastic phenotype? Mol Med Today. 1999;5(9):406-12.
37. Akhurst RJ, Derynck R. TGF-beta signaling in cancer - a double-edged sword. Trends in Cell Biology. 2001;11(11):S44-S51.
38. Kozlow W, Guise TA. Breast cancer metastasis to bone: mechanisms of osteolysis and implications for therapy. J Mammary Gland Biol Neoplasia. 2005;10(2):169-80.
39. Cicek M, Iwaniec UT, Goblirsch MJ, Vrabel A, Ruan M, Clohisy DR, et al. 2-Methoxyestradiol suppresses osteolytic breast cancer tumor progression in vivo. Cancer Res. 2007;67(21):10106-11.
40. O'Brien CA, Gubrij I, Lin SC, Saylors RL, Manolagas SC. STAT3 activation in stromal/osteoblastic cells is required for induction of the receptor activator of NF-kappaB ligand and stimulation of osteoclastogenesis by gp130-utilizing cytokines or interleukin-1 but not 1,25-dihydroxyvitamin D3 or parathyroid hormone. J Biol Chem. 1999;274(27):19301-8.
41. Whitehead KA, Dahlman JE, Langer RS, Anderson DG. Silencing or stimulation? siRNA delivery and the immune system. Annu Rev Chem Biomol Eng. 2011;2:77-96.
42. Jackson AL, Bartz SR, Schelter J, Kobayashi SV, Burchard J, Mao M, et al. Expression profiling reveals off-target gene regulation by RNAi. Nat Biotechnol. 2003;21(6):635-7.
43. Colucci S, Brunetti G, Rizzi R, Zonno A, Mori G, Colaianni G, et al. T cells support osteoclastogenesis in an in vitro model derived from human multiple myeloma bone disease: the role of the OPG/TRAIL interaction. Blood. 2004;104(12):3722-30.
44. Roato I, Grano M, Brunetti G, Colucci S, Mussa A, Bertetto O, et al. Mechanisms of spontaneous osteoclastogenesis in cancer with bone involvement. Faseb Journal. 2004;18(14):228-+.

45. Roato I, Gorassini E, Brunetti G, Grano M, Ciuffreda L, Mussa A, et al. IL-7 modulates osteoclastogenesis in patients affected by solid tumors. Skeletal Biology and Medicine, Pt B: Disease Mechanisms and Therapeutic Challenges. 2007;1117:377-84.
46. Tay JY, Bay BH, Yeo JF, Harris M, Meghji S, Dheen ST. Identification of RANKL in osteolytic lesions of the facial skeleton. J Dent Res. 2004;83(4):349-53.
47. Iguchi H, Yokota M, Fukutomi M, Uchimura K, Yonemasu H, Hachitanda Y, et al. A possible role of VEGF in osteolytic bone metastasis of hepatocellular carcinoma. Journal of Experimental & Clinical Cancer Research. 2002;21(3):309-13.
48. Naugler WE, Karin M. The wolf in sheep's clothing: the role of interleukin-6 in immunity, inflammation and cancer. Trends Mol Med. 2008;14(3):109-19.
49. Kumta SM, Huang L, Cheng YY, Chow LTC, Lee KM, Zheng MH. Expression of VEGF and MMP-9 in giant cell tumor of bone and other osteolytic lesions. Life Sciences. 2003;73(11):1427-36.
50. Willmarth NE, Ethier SP. Amphiregulin as a novel target for breast cancer therapy. J Mammary Gland Biol Neoplasia. 2008;13(2):171-9.
51. Qi CF, Liscia DS, Normanno N, Merlo G, Johnson GR, Gullick WJ, et al. Expression of transforming growth factor alpha, amphiregulin and cripto-1 in human breast carcinomas. Br J Cancer. 1994;69(5):903-10.
52. Panico L, D'Antonio A, Salvatore G, Mezza E, Tortora G, De Laurentiis M, et al. Differential immunohistochemical detection of transforming growth factor alpha, amphiregulin and CRIPTO in human normal and malignant breast tissues. Int J Cancer. 1996;65(1):51-6.
53. Gilmore JL, Scott JA, Bouizar Z, Robling A, Pitfield SE, Riese DJ, et al. Amphiregulin-EGFR signaling regulates PTHrP gene expression in breast cancer cells. Breast Cancer Res Treat. 2008;110(3):493-505.
54. Lu X, Wang Q, Hu G, Van Poznak C, Fleisher M, Reiss M, et al. ADAMTS1 and MMP1 proteolytically engage EGF-like ligands in an osteolytic signaling cascade for bone metastasis. Genes Dev. 2009;23(16):1882-94.
55. Morrison C, Mancini S, Cipollone J, Kappelhoff R, Roskelley C, Overall C. Microarray and Proteomic Analysis of Breast Cancer Cell and Osteoblast Co-cultures: ROLE OF OSTEOBLAST MATRIX METALLOPROTEINASE (MMP)-13 IN BONE METASTASIS. J Biol Chem. 2011;286(39):34271-85.
56. Beerli RR, Hynes NE. Epidermal growth factor-related peptides activate distinct subsets of ErbB receptors and differ in their biological activities. J Biol Chem. 1996;271(11):6071-6.
57. Chanda D, Isayeva T, Kumar S, Siegal GP, Szafran AA, Zinn KR, et al. Systemic osteoprotegerin gene therapy restores tumor-induced bone loss in a therapeutic model of breast cancer bone metastasis. Mol Ther. 2008;16(5):871-8.
58. Aranda PS, LaJoie DM, Jorcyk CL. Bleach gel: a simple agarose gel for analyzing RNA quality. Electrophoresis. 2012;33(2):366-9.
59. Bakewell SJ, Nestor P, Prasad S, Tomasson MH, Dowland N, Mehrotra M, et al. Platelet and osteoclast beta3 integrins are critical for bone metastasis. Proc Natl Acad Sci U S A. 2003;100(24):14205-10.
60. Eckhardt BL, Parker BS, van Laar RK, Restall CM, Natoli AL, Tavaria MD, et al. Genomic analysis of a spontaneous model of breast cancer metastasis to bone reveals a role for the extracellular matrix. Molecular Cancer Research. 2005;3(1):1-13.
61. Livak KJ, Schmittgen TD. Analysis of relative gene expression data using real-time quantitative PCR and the 2(-Delta Delta C(T)) Method. Methods. 2001;25(4):402-8.

DOI: 10.1177/1947601912458284

## FIGURE LEGENDS

**Figure 1.**

**OSM-induced invasive potential of mouse mammary tumor cells *in vitro*.** **A**, Secreted OSM levels (ELISA**)** from equal numbers of cells ($1x10^5$) and **B**, semi-quantitative expression of OSMRβ (RT-PCR, normalized to GAPDH expression) was compared between 66c14 and 4T1.2 mouse mammary tumor cells. **C**, Bone metastatic mammary tumor 4T1.2 cells were treated with 25 ng/ml OSM and show decreased adherent cell number over time (**left**) and increased cell detachment (**right**) when monitored for up to 10 days in culture. **D**, The percentage of 4T1.2 cells that migrated through Matrigel-coated transwell plates increased with 24-hour OSM treatment. Single chambers from 3 independent experiments were analyzed; data expressed as mean ± SEM, *$P < 0.05$, t-test.

**Figure 2.**

**4T1.2 cells with reduced OSM expression are less metastatic to bone.** **A**, 4T1.2 cells were transfected with shRNAs directed against the control LacZ or OSM (sequences 1-2), and secreted OSM was measured by ELISA in medium collected from wells containing $1 \times 10^5$ cells as well as RT-PCR (inset). **B**, Control 4T1.2-LacZ, 4T1.2-OSM1, or 4T1.2-OSM2 cells were injected into the $4^{th}$ mammary fat pad of female Balb/c mice and tumor growth was measured. Average tumor volume ($mm^3$) in control 4T1.2-LacZ, 4T1.2-OSM1, and 4T1.2-OSM2 cell-injected mice was monitored and significantly increased in 4T1.2-OSM2 mice at 30 days post-tumor cell injection compared to controls. **C**, 4T1.2-OSM1 and 4T1.2-OSM2, compared to control 4T1.2-LacZ injected mice, have significantly reduced spontaneous bone metastases as assessed by qPCR. **D**, Representative histology (H & E stain) shows a large intraosseous

metastasis in the vertebral pedicle of a 4T1.2-LacZ spine (n=2), a single small metastasis in the outside edge of the vertebral body of a 4T1.2-OSM1 spine, and only normal osseous tissue in 4T1.2-OSM2 spine (n=2). (4T1.2-LacZ, n=22; 4T1.2-OSM1, n=14; 4T1.2-OSM2, n=22). Data expressed as mean ± SEM, *P < 0.05; (A) One-way ANOVA with Tukey's post-hoc test, (B and D) t-test.

**Figure 3.**

**Reduced OSM expression by 4T1.2 cells protects against bone osteolysis.** **A**, Representative 3D reconstructions of hind limbs were generated from Micro CT scans performed 4 weeks after intratibial injection of PBS, control 4T1.2-LacZ cells, or 4T1.2-OSM2 cells. Insets show extensive osteolysis in the proximal tibia of mice injected with control cells. **B**, ROI 3D reconstructions of trabecular (**top**) and cortical bone (**bottom**) show less osteolytic degradation in tibias injected with 4T1.2-OSM2 cells compared to control cells. **C**, Quantitative analyses were performed for total trabecular volume, total trabecular thickness, cortical bone volume/total volume, and cortical bone mineral density. (PBS, n=2; 4T1.2-LacZ, n=3; 4T1.2-OSM2, n=4). Data expressed as mean ± SEM. *P<0.001, t-test 4T1.2-OSM2 vs 4T1.2-LacZ. BDL (below detection limit) is presented when no data could be obtained and resulted in the inability to perform statistics.

**Figure 4.**

**Reduced OSM expression by 4T1.2 tumors increases survival.** **A**, The timeline shows orthotopic mammary tumor cell injection at day 0, resection at day 14, and final day of sacrifice per group. **B**, Kaplan-Meier analysis of survival following tumor resection shows a significant

increase in survival in mice injected with 4T1.2-OSM2 cells. **C**, Relative metastatic burden for spine was also significantly lower in the 4T1.2-OSM2 injected mice as assessed by qPCR. (4T1.2-LacZ, n=6; 4T1.2-OSM2, n=10). Data expressed as mean ± SEM. **P<0.01, Log-rank test, ***P<0.001, t-test.

**Figure 5**

**OSM induces 4T1.2 tumor cell-mediated osteoclastogenesis *in vitro*.** **A**, Expression of various receptors on mouse 4T1.2 and RAW 264.7 cells was analyzed by RT-PCR (normalized to GAPDH expression). **B**, 10-day treatment with 25 ng/ml of OSM increases the number of TRAP+ cells in RAW 264.7 and 4T1.2 cell co-cultures and RAW 264.7 cells treated with 4T1.2 cell CM. **C**, OSM induces IL-6 and **D**, VEGF secretion in 4T1.2 cells and co-cultures of RAW 264.7 and 4T1.2 cells, measured by ELISA (total of 1 x $10^5$ cells per well). *P < 0.05; ***P<0.001, Two-way ANOVA with Boneferroni post-hoc test.

**Figure 6.**

**OSM-induced AREG secretion drives 4T1.2 cell-mediated osteoclastogenesis *in vitro*.** **A**, The amount of AREG secreted by 4T1.2 cells, co-cultures of 4T1.2 and RAW 264.7 cells, or RAW 264.7 cells alone (total of 1 x $10^5$ cells) increases after 48-hour treatment with 25 ng/ml OSM, as analyzed by ELISA (**left**). 10-day recombinant AREG (50 ng/ml) and OSM (25 ng/ml) treatment increases the number of TRAP+ cells in co-cultures of RAW 264.7 and 4T1.2 cells (**right**). **B**, Addition of a neutralizing antibody against AREG (1 μg/ml anti-AREG) 2 hours prior to OSM treatment blocks the increase in the number of OSM-induced TRAP+ cells (**left**). A comparison of the percent increase in TRAP+ cells (% of -OSM Control) in co-cultures of

RAW 264.7 and 4T1.2 cells treated with neutralizing antibodies directed against IL-6 (anti-IL-6, 1 μg/ml), VEGF (anti-VEGF, 1 μg/ml), and anti-AREG (1 μg/ml) 2 hours prior to the addition of OSM is shown (**right**). **C**, OSM inhibits OPG secretion levels, as assessed by ELISA (**left**). OSM and AREG inhibit OPG mRNA expression by RT-PCR (normalized to GAPDH) (**right**). *P < 0.05, ***P<0.001; Two-way ANOVA with Boneferroni post-hoc analysis (A and B, left);***P<0.05, **P<0.01, ***P<0.001; One-way ANOVA with Tukey's post-hoc analysis (B, right, + OSM groups); *P < 0.05; Unpaired t-test (C).

**Figure 7.**

**Proposed model for the mechanism of OSM in tumor cell-mediated osteoclastogenesis.**

OSM increases VEGF and IL-6 secretion from tumor cells that then bind to pre-osteoclasts and mature osteoclasts on their respective VEGF and IL-6 receptors (VEGFR and IL-6R) to promote osteoclastogenesis and osteoclast activity in the presence of RANKL and M-CSF, resulting in bone resorption. OSM also induces tumor cell-secreted AREG that signals via an unknown receptor to suppress OPG production and reduce its ability to bind RANKL and inhibit osteoclastogenesis. Thus membrane-bound RANKL on osteoblasts or soluble RANKL (sRANKL) is more available to bind to RANK on pre-osteoclasts, thereby promoting osteoclastogenesis. cFMS; receptor for M-CSF.

**Figure 1**

**Bolin and Tawara et. al.**

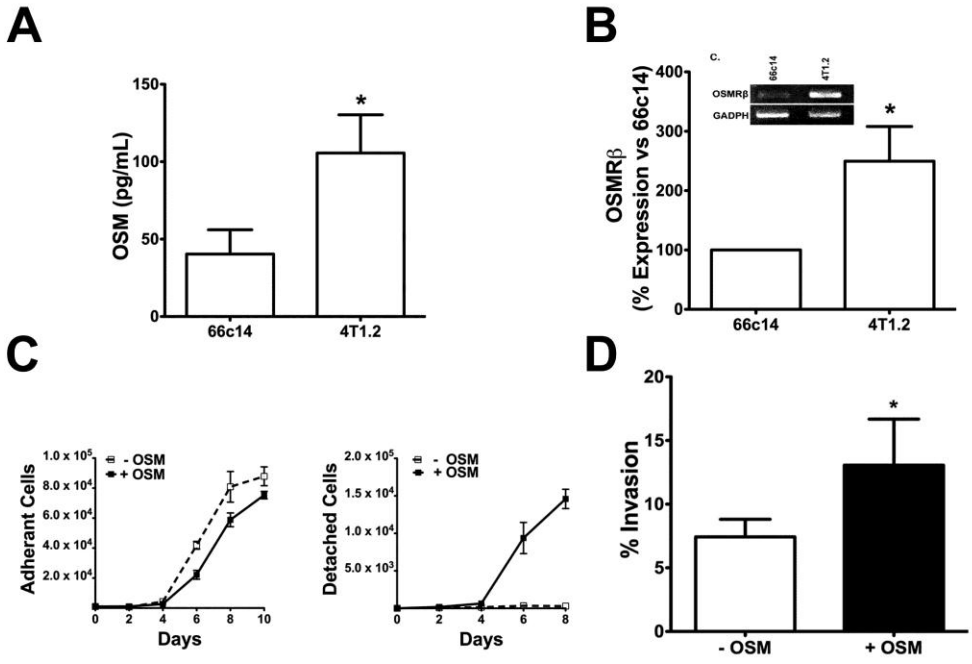

**Figure 2**

**Bolin and Tawara et. al.**

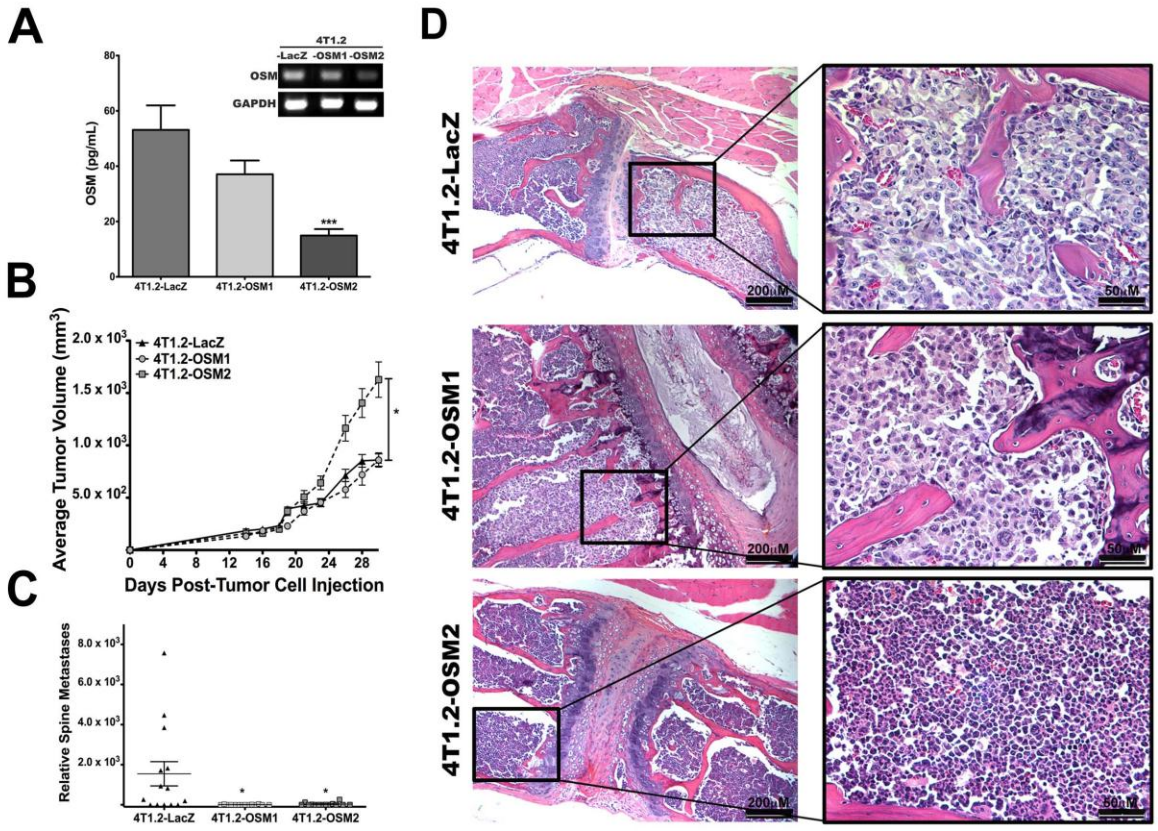

**Figure 3** **Bolin and Tawara et. al.**

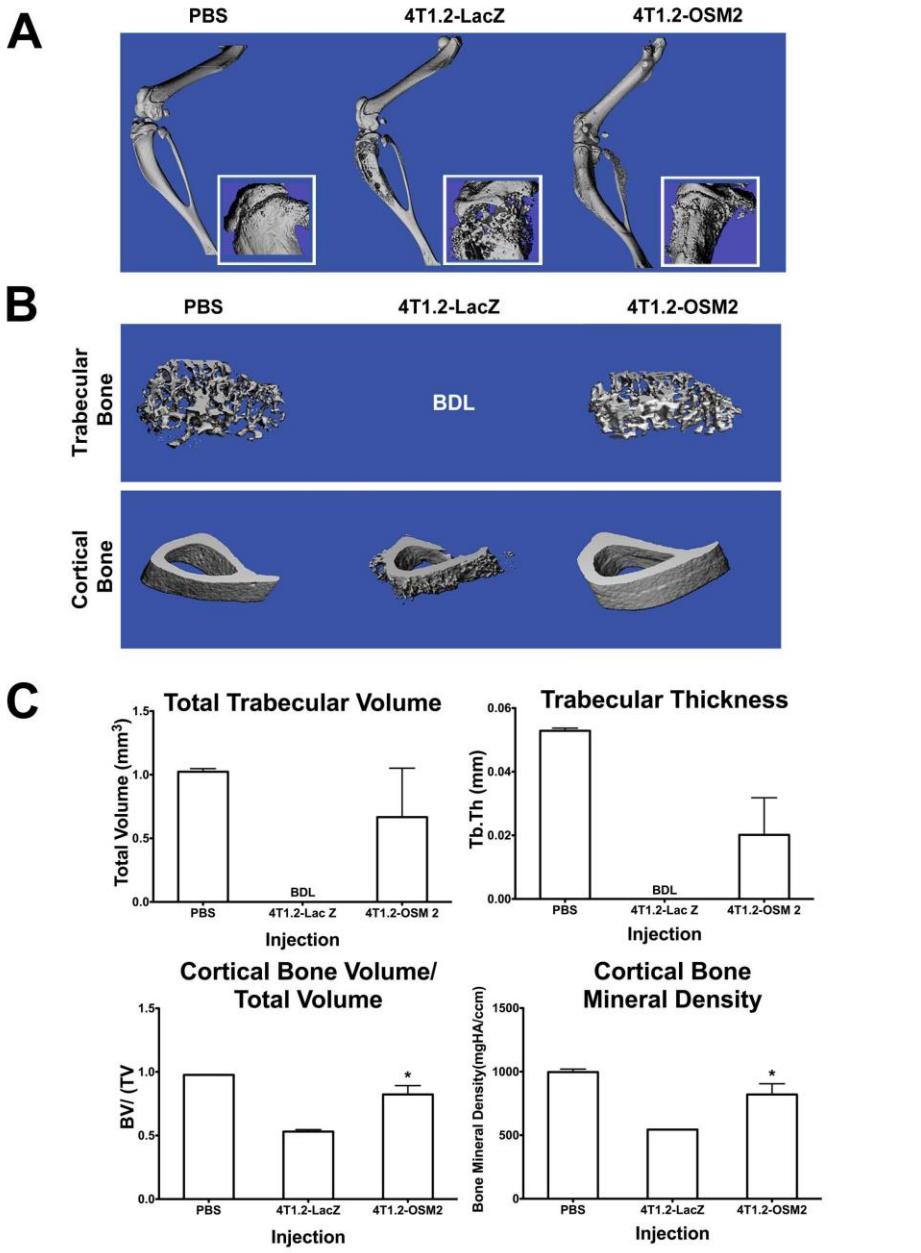

**Figure 4** **Bolin and Tawara et. al.**

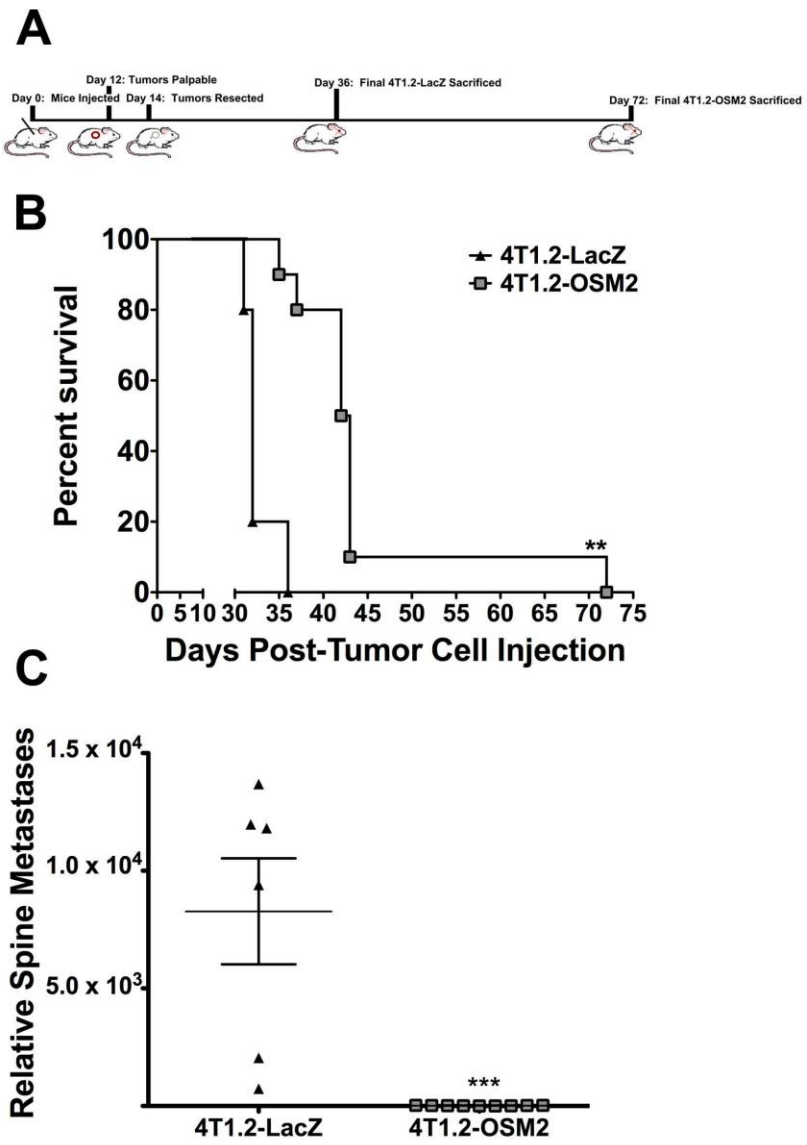

**Figure 5**

**Bolin and Tawara et. al.**

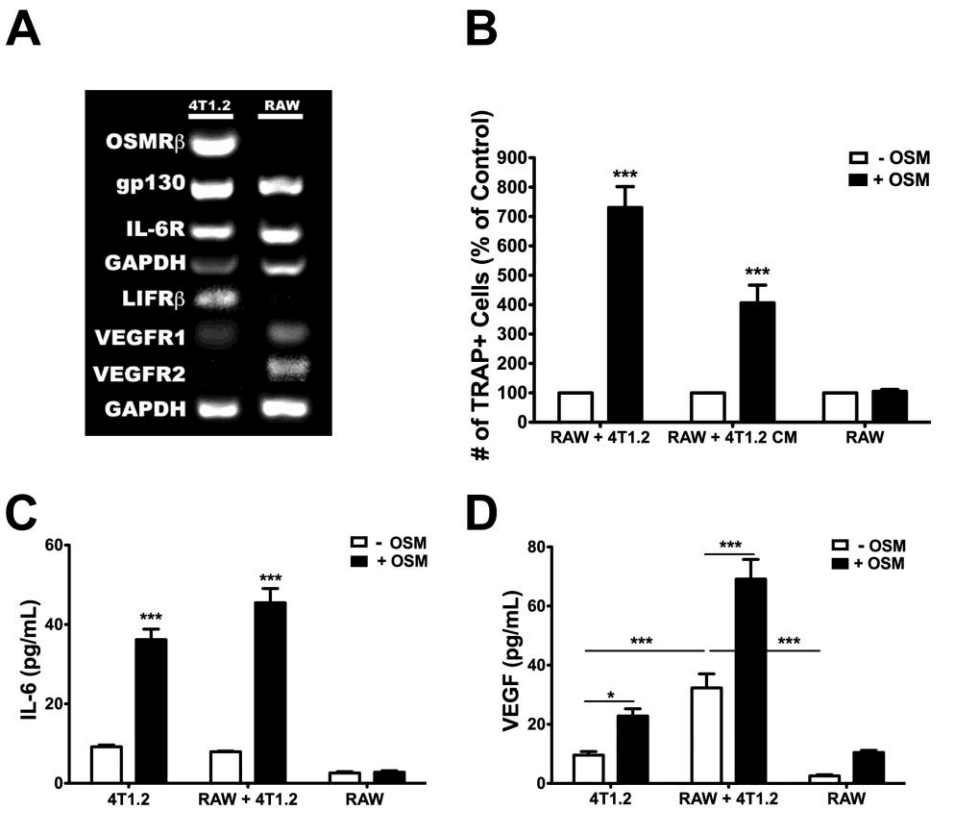

**Figure 6** **Bolin and Tawara et. al.**

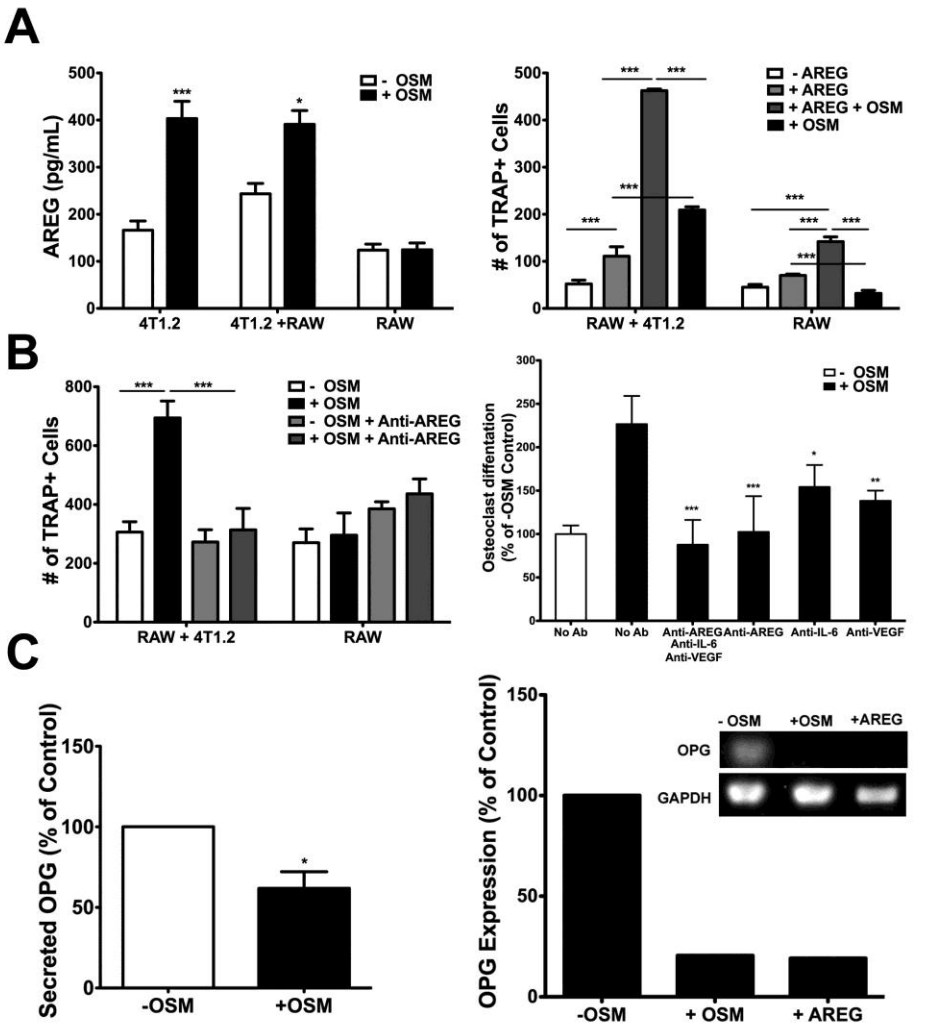

**Figure 7** **Bolin and Tawara et. al.**

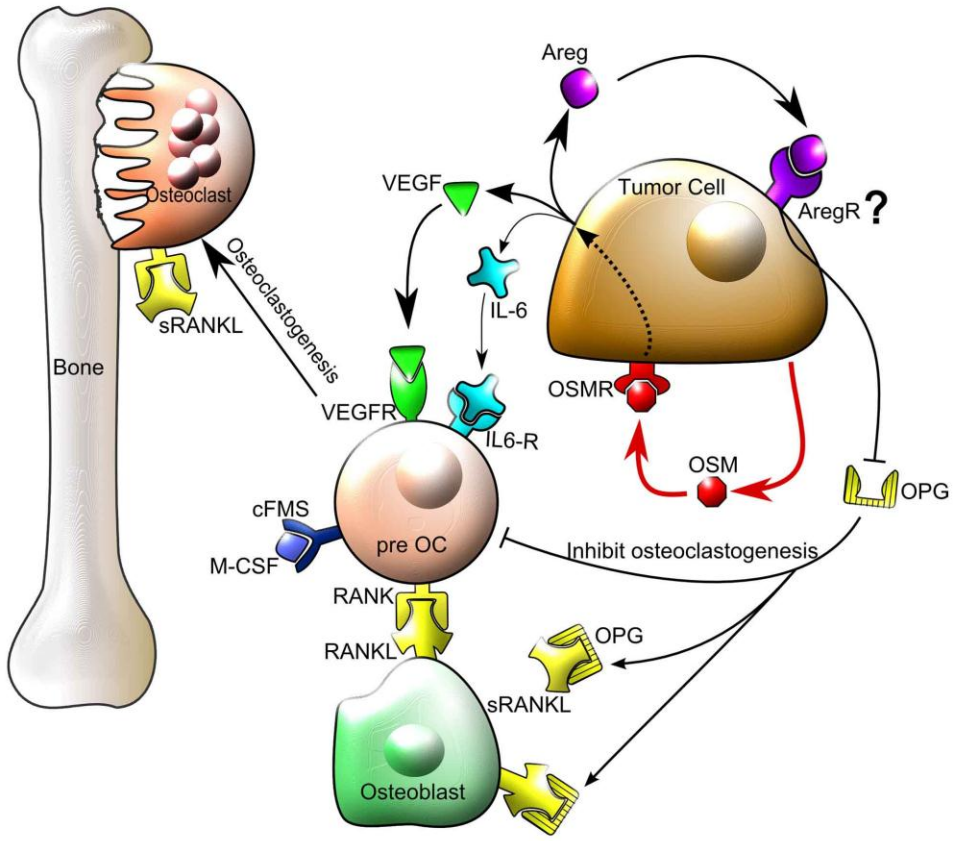

**Supplemental Table 1** **Bolin and Tawara et. al.**

**Supplementary Table 1. Sequence of qPCR and RT-PCR Primers**

**qPCR Primer Sequences**

| Gene | Function | Forward Primer Sequence (5'-3') | Reverse Primer Sequence (5'-3') |
|---|---|---|---|
| Neomycin | Primer | GCGCCCGGTTCTTTTTG | CCTCGTCCTGGAGTTCATTCA |
| | Probe | 6FAM-CAAGACCGACCTGTCCGGTGCC-TAMRA | |
| Vimentin | Primer | AGCTGCTAACTACCAGGACACTATTG | CGAAGGTGACGAGCCATC |
| | Probe | VIC-CCTTCATGTTTTGGATCTCATCCTGCAGG-TAMRA | |

**RT-PCR Primer Sequences**

| Gene | Annealing Temp ($T_A$) | Forward Primer Sequence (5'-3') | Reverse Primer Sequence (5'-3') | Product Length (bp) |
|---|---|---|---|---|
| OSM | 59.5 | AGCAAGCCTCACTTCCTGAG | GTGGGCTCAGGTATCTCCAG | 200 |
| OSMRb | 60 | TAGACTGAACATATCCAACACCA | TCCATGGATTGGCTCATCTGGCA | 349 |
| gp130 | 58 | CGTACACAGATGAAGGTGGGAAAG | CTTCAGGCTGACTGCAGTTCTGC | 691 |
| IL-6R | 60 | CCAGGTGCCCTGTCAGTATT | CCGTGAACTCCTTTGACCAT | 317 |
| GAPDH | 57 | GGTCCTCAGTGTAGCCCAAG | ATCACTGCCACCCAGAAGAC | 202 |
| LIFRb | 52 | GAAAACTGTAAGGCGCTACA | CCAAGTGTTTACATTGGC | 483 |
| EGFR | 57 | AGCAAGGCTTCTTCAACAGC | AGACAGGTAGGCTGGGCAGT | 376 |
| VEGFR1 | 55 | TTCTGTCCTCCAGAAAGTGC | ATCCATTTTAGGGGAAGTCG | 163 |
| VEGFR2 | 63 | AGCTTGGCTCACAGGCAACATCGG | TGGCCCGCTTAACGGTCCGTAGG | 624 |
| Areg | 55 | GCGAATGCAGATACATCGAGAA | TCCACACCGTTCACCAAAGTAA | 77 |
| ADAMTS1 | 63 | GGCGCCCCACGGAGGAAG | AGGCGCTGGCTGAATGAAGAAC | 347 |
| HIF1a | 55 | GCACTAGACAAAGTTCACCTGAGA | CGCTATCCACATCAAAGCAA | 105 |
| OPG | 55 | TGAGTGTGAGGAAGGGCGTTA | CCATCTGGACATTTTTTGCAAA | 129 |
| IGF1 | 47 | CACCTTGCA AAAGTGGTCCT | AGCTACGTGGGA AGAGGTGA | 220 |
| IGF2 | 52 | CCTCTTGAGCAGGGACAGT | GGGTGTCAATTGGGT TGT TT | 200 |
| IGF2R | 59.5 | GTGTCCTCTGGGTGTGGACT | CTCCTCCTTGCTGACCTTTG | 241 |

**Supplemental Table 2**

**Bolin and Tawara et. al.**

**Supplementary Table 2. Regulation of Breast Cancer to Bone Metastatic Factors by OSM**
R: RT-PCR, W: Western Blot, E: ELISA, PA: Protein Array

| Gene/Protein Type | Gene/Protein | Assay Type | Modulation by OSM in 4T1.2 Cells |
|---|---|---|---|
| **Tumor Secreted Factors** | IL-6 | E | → |
| | OSM | R | — |
| | AREG | E, R | ↑↑ |
| | ADAMTS1 | R | → |
| **Pro-Angiogenic Factors** | VEGF | E | → |
| | VEGFR1 | R | — |
| | VEGFR2 | R | — |
| **Bone Homeostasis Factors** | RANK L | W | — |
| | M-CSF | E | — |
| | OPG | E,R | ← |
| | PTHrP | E | — |
| | Osteopontin | PA | — |
| **Metastatic Factors** | IGF1/IGF2 | R | — |
| | IGF2R | R | — |
| | TNF alpha | E | — |
| | TGF beta | E | — |

**Supplemental Figure 1**

**Bolin and Tawara et. al.**

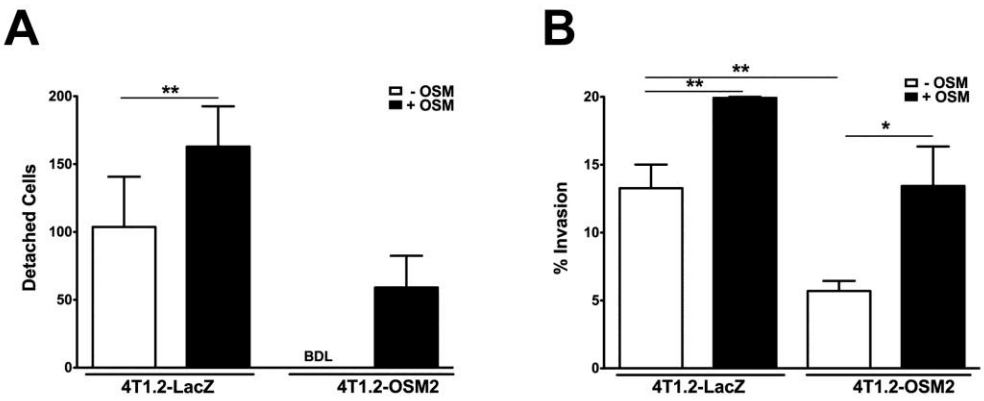

**Supplemental Figure 2**

**Bolin and Tawara et. al.**